THESIS FOR DEGREE OF MASTER OF SCIENCE

Mutation of *SPOTTED LEAF4 (SPL4)* encoding a microtubule severing protein produces reactive oxygen species (ROS) and delays leaf senescence in rice

벼의 미세소관 절단 단백질을 암호화하는 *SPL4* 돌연변이체에서의 활성산소 생성과 잎의 노화 지연

BY

GIHA SONG

FEBRUARY, 2017

MAJOR IN CROP SCIENCE AND BIOTECHNOLOGY

DEPARTMENT OF PLANT SCIENCE

THE GRADUATE SCHOOL OF SEOUL NATIONAL UNIVERSITY

Mutation of *SPOTTED LEAF4 (SPL4)* encoding a microtubule severing protein produces reactive oxygen species (ROS) and delays leaf senescence in rice

UNDER THE DIRECTION OF DR. NAM-CHON PAEK
SUBMITTED TO THE FACULTY OF THE GRADUATE SCHOOL
OF SEOUL NATIONAL UNIVERSITY

BY
GIHA SONG

MAJOR IN CROP SCIENCE AND BIOTECHNOLOGY
DEPARTMENT OF PLANT SCIENCE

NOVEMBER, 2016

APPROVED AS A QUALIFIED DISSERTATION OF GIHA SONG
FOR THE DEGREE OF MASTER
BY THE COMMITTEE MEMBERS

FEBRUARY, 2017

CHAIRMAN

Hee-Jong Koh, Ph.D.

VICE-CHAIRMAN

Nam-Chon Paek, Ph.D.

MEMBER

Tea-Jin Yang, Ph.D.

Mutation of *SPOTTED LEAF4 (SPL4)* encoding a microtubule severing protein produces reactive oxygen species (ROS) and delays leaf senescence in rice

GIHA SONG

ABSTRACT

The mutants show autonomous lesion formation, spontaneous cell death without any pathogen attack and resistance to a pathogen are classified to lesion mimic mutants (LMMs). Through these phenotypes, LMMs were used to study the mechanisms of programmed cell death pathway and response to a pathogen. In this study, the *spotted leaf4 (spl4)* mutant which is derived from γ-ray irradiation were used to study the spontaneous cell death mechanism. It has been reported that many LMMs its encoding genes were identified but its molecular mechanism of lesion formation and pathogen resistance is still unclear. The reactive oxygen species (ROS) is the product of senescence and ROS can be found near the spots in LMMs during autonomous lesion formation in LMMs even dough it is a developmental stage. Stay-green is the phenomena of delayed senescence and this is the one character that breeders want to achieve. Also, Scientists study this delayed senescence phenotype to elucidate the leaf senescence mechanism. In this study, we

analyzed the rice *spl4* mutant, which shows autonomous lesion formation on leaf blades, ROS accumulation and shows the stay-green phenotype. The *spl4* locus was identified by map-based cloning. This locus encodes a putative microtubule severing protein, spastin. Our data may suggest that the malfunctioning of microtubule severing protein results in pleiotropic phenotypes of autonomous lesion formation, ROS accumulation and delayed senescence in *spl4* mutant.

Keywords: rice, *SPOTTED LEAF4 (SPL4)*, lesion mimic mutant, reactive oxygen species, leaf senescence

Student number: 2015-21487

CONTENTS

ABSTRACT ····· i

CONTENTS ····· iii

LIST OF FIGURES ····· iv

LIST OF TABLES ····· v

ABBREVIATION ····· vi

INTRODUCTION ····· 1

MATERIALS AND METHODS ····· 4

RESULTS ····· 11

DISCUSSION ····· 31

REFERENCES ····· 36

ABSTRACT IN KOREAN ····· 41

LIST OF FIGURES

Figure 1. Phenotypic characterization of the *spl4* mutant

Figure 2. Early phenotypic characterization of the *spl4* mutant

Figure 3. Tillering and heading stage phenotypic characterization of the *spl4* mutant

Figure 4. ROS accumulation in *spl4* mutant

Figure 5. Stay-green phenotype of *spl4*

Figure 6. Yield-related agronomic traits of the *spl4* mutant

Figure 7. Map-based cloning of *spl4*

Figure 8. Subcellular localization of SPL4

Figure 9. Protein expression of SPL4

Figure 10. ATPase activity of GST-SPL4

LIST OF TABLES

Table 1. Information of primers used in this study

Table 2. Yield-related agronomic traits of the *spl4* mutant

ABBREVIATION

LMM	Lesion mimic mutant
ROS	Reactive oxygen species
MAP	Microtubule-associated protein
NLD	Natural long day
DAB	3,3'-diaminobenzidine
SOSG	Singlet oxygen sensor green
GST	Glutathione S-transferase
CBB	Coomassie brilliant blue
STS	Sequence-tagged-site
WT	Wild-type
MIT spastin	Microtubule-interacting and trafficking spastin
AAA+	ATPase associated with wide various of cellular activities
DAPI	4',6-diamidino-2-phenylindole
DIC	Differential interference contrast
MAPKKK	Mitogen-activated protein kinase kinase kinase
MAPKK	Mitogen-activated protein kinase kinase
MAPK	Mitogen-activated protein kinase

INTRODUCTION

The lesion mimic mutant (LMM) is one of the categorized mutants which shows autonomous lesions and spontaneous cell death without any pathogen attack. Except for autonomous lesion, another well-known phenotype of LMM is the resistance to pathogen [1-4]. These phenotypes have provided a way to study the mechanisms of programmed cell death and pathogen response. Many LMMs has been isolated from various species, such as barley [5], maize [6], Arabidopsis [7] and rice [8]. Especially in Oryza sativa, several LMMs have been identified and the isolated genes encode coproporphyrinogen III oxidase (CPOX) [9, 10], uroporphyrinogen decarboxylase protein (UROD) [11], Mitogen-Activated Protein Kinase Kinase Kinase1 (MAPKKK1) [8, 12, 13], a clathrin-associated adaptor protein complex 1, medium subunit μ1 (AP1M1) [4], U-Box/Armadillo Repeat Protein [14], and a heat stress transcription factor protein [15].It indicates that various genes are involved in lesion formation of LMMs in rice and its molecular mechanism is still complicated and unclear.

Almost LMMs show reactive oxygen species (ROS) accumulation during autonomous lesion formation. It has been reported that the hydrogen peroxide (H_2O_2) which is one of the ROS induces apoptosis in both plant and mammal [16, 17]. Accumulation of ROS leads to the cell death, resulting in the lesion formation on leaves [18, 19]. In addition, the ROS can be induced

by senescence [20]. All organisms are face to aging through lifetime and the ROS necessarily accumulates during the senescence. Delayed senescence, in other words, the stay green, is one of the phenotypes that we want to achieve into the crop. This remarkable phenotype is expected to increase the crop yield [21]. Also, this phenotype is one of the ways to study leaf senescence mechanism. There are five types of stay green phenotypes which are type A to E [22]. According to previous research, the functional stay green type A and B showed delayed initiation of leaf senescence and a slower rate of leaf senescence respectively. The other types of stay green, type C showed declined activity of photosynthesis with delayed chlorophyll degradation, type D showed cell dying in the middle of the leaf senescence and lastly type E showed higher chlorophyll contents overall whole lifetime [22].

Microtubule is one of the main structural components of the cytoskeleton with microfilaments and intermediate filaments. The α and β-tubulin polymerize to form a dimer and these dimers are the basic components of the microtubule. In the previous study, the microtubule was known to involved in cell division [23], morphogenesis [24] and migration [25]. In cell biology, the proteins which interact with microtubule are called microtubule-associated proteins (MAPs). The motor protein, kinesin, and dynein are the one of the MAP. These motor proteins can transform the ATP hydrolysis energy to mechanical movement so that these motor proteins can move along the microtubule [26]. Kinesin and dynein move along the microtubule by anterogradely and retrogradely respectively [27]. These motor proteins carry

the cargo proteins especially scaffolding proteins to assembling the signal protein complex [28]. Through motor protein-cargo protein complex the signals in the cell can spread to target site not only with cytosol diffusion [29]. Consequently, the microtubule is involved in signal transduction in the cell because of the movement of motor proteins are determined by microtubule.

As mentioned above, microtubule has to be regulated because of its act as a road of signal transduction. The microtubule-severing proteins are the one identified microtubule-regulating proteins. Thus far, the three microtubule severing proteins were identified. These are katanin [30], spastin [31] and fidgtin [32]. In the previous study, katanin and spastin are showing the different working model to microtubule [33]. In human, almost 40% of Hereditary spastic paraplegias (HSP) which is inherited the disease, is caused by a mutation in the spastin protein [34]. Studies on microtubule severing proteins are still on-going and most of them are largely unknown. However, these microtubule severing proteins are almost involved in animal nerve system [30-32]. In this study, we analyzed the rice *spl4* mutant, which produces autonomous lesions on leaf blades and shows the stay-green phenotype. By map-based cloning, we revealed *spl4* locus encodes a putative microtubule severing protein, spastin. Malfunctioning of spastin results in pleiotropic phenotypes of spontaneous cell death and delayed senescence in the time of plant life. We believe that this isolation of *spl4* gene would provide more information to LMMs and also in plant cytoskeleton system.

MATERIALS AND METHODS

Plant materials and growth conditions

The single recessive mutant *spl4* was derived from Japanese japonica rice cultivar 'Norin8' by γ-ray irradiation [35]. The wild-type (WT) Norin8 and *spl4* were grown in the paddy field (natural long day (NLD) conditions at 37˚N latitude, Suwon, Korea) or in the growth chambers. The chamber experiments were performed under short-day (SD) conditions [10-h light with normal intensity (300 $\mu molm^{-2}sec^{-1}$) at 30℃ and 14-h dark at 24℃]. For phenotypic characterization and map-based cloning of *spl4*, all the plants were grown in the NLD paddy field. The T-DNA insertion mutant of *spl4* (PFG_3A-16679.R) was isolated in the Korean japonica cultivar ‘Dongjin’ [36, 37].

Detection of ROS

To determine hydrogen peroxide (H_2O_2), leaf samples of 60, 70, 80 and 125 days after sowing plants grown in the paddy field were transferred in 3,3'-diaminobenzidine (DAB) staining solution containing 0.1% 3,3'-diaminobenzidine in 50 mM sodium phosphate buffer, and incubated for 3h with gentle shaking. After staining, chlorophyll was completely removed by incubation with 95% ethanol at 80℃. For singlet oxygen staining, 133 days after sowing plants grown in the paddy field were immersed into 50mM Singlet

oxygen sensor green (SOSG) in 10mM sodium phosphate buffer (pH 7.5). After incubation in dark for 30 min, analyzed on Carl Zeiss confocal laser scanning microscope (LSM710, Germany) installed at the National Center for Inter-university Research Facilities (NCIRF) at Seoul National University.

Purification of recombinant protein

The full-length cDNA of *spl4* was cloned into the pGEX 4T-1 protein expression vector to examine *spl4* ATPase activity. Recombinant proteins produced in E.coli (R2) were fused to Glutathione S-transferase (GST). The cells were grown at 37℃ into the exponential growth phase, then cooled down to 20℃, and protein production was induced with 0.1mM Isopropyl β-D-1-thiogalactopyranoside (IPTG). Cells were harvested after 4h. For purification of GST-tagged SPL4, E.coli were resuspended in GST binding buffer (25mM Tris, pH 7.5, 150mM NaCl, 1mM EDTA) and sonicated. The lysate was centrifuged at 13,000g for 30min and 4℃. The supernatant was incubated with GST-bind agarose resin for 1h at 4℃. The flow through was discarded and the resin washed with GST binding buffer until the flow through was clear of protein. GST fusion proteins were eluted with elution buffer (15mM reduced glutathione, 1mM EDTA, 50mM Tris, pH 9.6).

SDS-PAGE and immunoblot analysis

Preparation of flow through samples, SDS-PAGE and western blot analysis were performed using coomassie brilliant blue (CBB) gel staining and mouse anti-GST. The predicted molecular weight of the recombinant protein was 79 kDa.

Rice protoplast preparation and subcellular localization

Rice protoplast prepared from 10~15 day-old etiolated Dongjin rice seedlings. The etiolated stem and sheath tissues were transferred to a digestion solution consisting of 0.5M mannitol, 10mM MES pH 5.7, 1.5% (w/v) Cellulase R-10 (yakult pharmaceutical IND. CO., LTD., Japan), 0.75% (w/v) Macerozyme R-10 (yakult pharmaceutical IND. CO., LTD., Japan), 0.1% (w/v) BSA, 10mM CaCl2 and 5mM β-mercaptethanol. Tissues were vacuum infiltrated for 10min and digested for 4.5h in gentle shaking (40rpm) at 28℃.

Following enzymatic digestion, the protoplasts were released with the 20ml W5 solution. After filtration through a 70 and 40μm cell filter, isolated protoplasts were recovered by centrifugation for 8min (320 x g) at room temperature. Protoplasts were then resuspended in MMG solution (0.5M Mannitol, 15mM MgCl2, 4mM MES pH 5.7), quantified by counting using an hemocytometer, and their concentration adjusted to 1~10 x 10^7 cells/ml with MMG solution. For PEG-mediated transformation, 50μl of cells were incubated with 15μg of pMDC43-OsSPL4 (or empty vector for control) and

113ul of 40% (w/v) PEG solution (0.2M Mannitol, 100mM CaCl2, 40% (w/v) PEG 4000 (Fluka, Germany) for 12min at 28℃ in the dark. PEG solution was added to a 1ml W5 solution and the mixture centrifugation for 3min (300 x g). The transformed protoplasts were resuspended in 1.5ml incubation solution (0.5M Mannitol, 20mM KCl, 4mM MES pH 5.7) and transferred to 96-well plates. The transformed cells were incubated for 6-15h at room temperature in the dark. For subcellular localization, the cDNA of OsSPL4 was cloned into a pEG101 vector. After transformation, pEG101-OsSPL4 and empty vector for control were bombarded into onion epidermal layers using a DNA particle delivery system (Biolistic PDS-1000/He, BioRad), and incubated on MS solid medium for 16–18h at 23℃ under dark. Each incubated rice protoplast and onion epidermal layers were analyzed on Carl Zeiss confocal laser scanning microscope (LSM710, Germany) installed at the National Center for Inter-university Research Facilities (NCIRF) at Seoul National University, respectively.

Chlorophyll measurement

For the measurement of total chlorophyll concentration, photosynthetic pigments were extracted from the leaf tissues with 80% ice-cold acetone. Chl concentrations were determined by spectrophotometry as described previously [38]. The chlorophyll efficiency of photosystem II and chlorophyll

density can be measured with Fv/Fm ratio and SPAD value.

ATPase assay

ATPase assays were carried out for 30 min at Room temperature according to the manufacturer's instructions (Innova Biosciences). To evaluate the ATPase activity, elution products were incubated in substrate buffer containing 0.5mM ATP. Each assay was incubated for maximum 30 min and the reaction was stopped by adding 50μl PicolorLock with 0.5μl accelerator. Absorbance 620nm were used to read the sample absorbance. Standard curves of phosphate standards were according to the manufacturer's instructions (Innova Biosciences).

Map-based cloning and fine mapping

For genetic analysis, *spl4* mutant and Milyang23 (a tongil-type indica/japonica hybrid cultivar) crossed F2 plants were developed. The *spl4* locus was previously mapped to the short arm of chromosome 6 [35]. In this study, a mapping population of 898 F2 individuals from the cross between *spl4* and Milyang23 was used for locating and fine mapping of the *spl4* locus. Genomic DNA was extracted from young leaves of each F2 individual line. The newly designed markers using whole genome sequence data were used to narrow down the genomic region of *spl4* locus on chromosome 6; these markers included sequence-tagged-site (STS) markers (Table 1).

Table1. Information of primers used in this study.

Marker	Forward primer (5'→3')	Reverse primer(5'→3')
A. Primers used for map-based colning		
RM508	GGATAGATCATGTGTGGGGG	ACCCGTGAACCACAAAGAAC
STS1	AGCTCAATATCAGGCAAGCAG	AAATGACACAGTTGACCTTTTGAA
RM587	ACGCGAACAAATTAACAGCC	CTTTGCTACCAGTAGATCCA
RM510	AACCGGATTAGTTTCTCGCC	TGAGGACGACGAGCAGATTC
STS2	ATAGCAGGGTTGCCTTCTCA	GGGGCCATAACCCTAGACAT
RM276	CTCAACGTTGACACCTCGTG	TCCTCCATCGAGCAGTATCA
RM136	GAGAGCTCAGCTGCTGCCTC	GAGGAGCGCCACGGTGTACG
RM527	GGCTCGATCTAGAAAATCCG	TTGCACAGGTTGCGATAGAG
STS3	CCCCTTCATCATTGCAACTT	AGTCTCTCCATCACCCGTCT
STS4	CGTCGTACCCCTCATGTCTT	CACGCAATCTGTGTAATTAGTTTTT
RM3	ACACTGTAGCGGCCACTG	CCTCCACTGCTCCACATCTT
STS5	TAATGGTTGCAATGGGGCCT	GGCATAGTGCTCCTCTAGGC
RM6395	CTTCGGCTTCTGAACTAGCG	CAGTGCCGATGATCCTCTTC
RM528	GGCATCCAATTTTACCCCTC	AAATGGAGCATGGAGGTCAC
RM30	GGTTAGGCATCGTCACGG	TCACCTCACCACACGACACG
RM5753	AACATGCTCAACTTCTGGGC	GCTAGGTACGATCCAGCTGC
STS6	ATCAGAGTGAGGTAATCTGGACC	ACCATTTGATTTAGGTATATGAA
STS7	TAATGTCTTGGGTTGGGAATGGC	ATGCACTGCTCTGGCACACAAGT
STS8	GATTCATACCTTCACTTTGCGAT	AGCAAACTATGCAACTAACTGCA
STS9	TCAGTGTCCTTTGAACCATCTCAT	CTGCAGAAATGAAGTGACAGTTA
STS10	TGGATTAGTTCATTG32212.0TGCTATGA	AGAAGATGTCTTCGTCAGAGTTCT
STS11	AAGTATTAGCGTTAGTCGCCGG	TTGAAACAGTTTGACTTTGACCA
STS12	AAACTGGAGCAGATAACATGGCA	AGGATCGCATTGCACCGCTAGCT
STS13	ACCTTTCAGGAGCTATACCATTTGG	AAGTTTAGTTGATGCTTCCTTTTGT
B. Primers used for gene cloning		
spl4	ATGAGCTTCCTCCGCGCGCTCGCG	ACTTGAACCAAATTCTTCGTTCC
spl4-short	TTCGAGCTGGCCAAGGAGGAGATC	TGCGGCTCTGTCATTCCTATTAAC
spl4-protein	GGATCCATGAGCTTCCTCCGCGCG	GAATTCACTTGAACCAAATTC

C. Primers for verification of *spl4* T-DNA insertion		
PFG 3A-16679.R	GCATTTTTAAAGCGTGGAGC	GATCTTGAAAGGCTTGCTGC
D. Primers used for qRT-PCR		
spl4	TGATCTTGAAAGGCTTGCTGCAG	GCTTGGCCTAATCACAGTCATGG

RESULTS

A spontaneous lesion and defective phenotype of *spl4* mutant in natural paddy field

At the early vegetative stage, the *spl4* mutant showed a rolling phenotype in natural paddy field (Fig. 2A, B). In addition, the leaf width between WT and *spl4* had a difference at early developmental phase (Fig. 2C, D). However, this rolled leaf phenotype was rescued after about 74 days after sowing (Fig. 2E, F, G). The most striking phenotype of *spl4* was autonomous lesion formation from the second leaves at the end of tillering stage, while no spots on WT leaves (Fig. 1A, B). As the plants were in heading stage, autonomous lesions on *spl4* were more severe from the second leaves to older leaves, except flag leaves (Fig. 1C, D). During the whole growth period, the height of *spl4* mutant was shorter than that of WT (Fig. 1A, C, E, H).

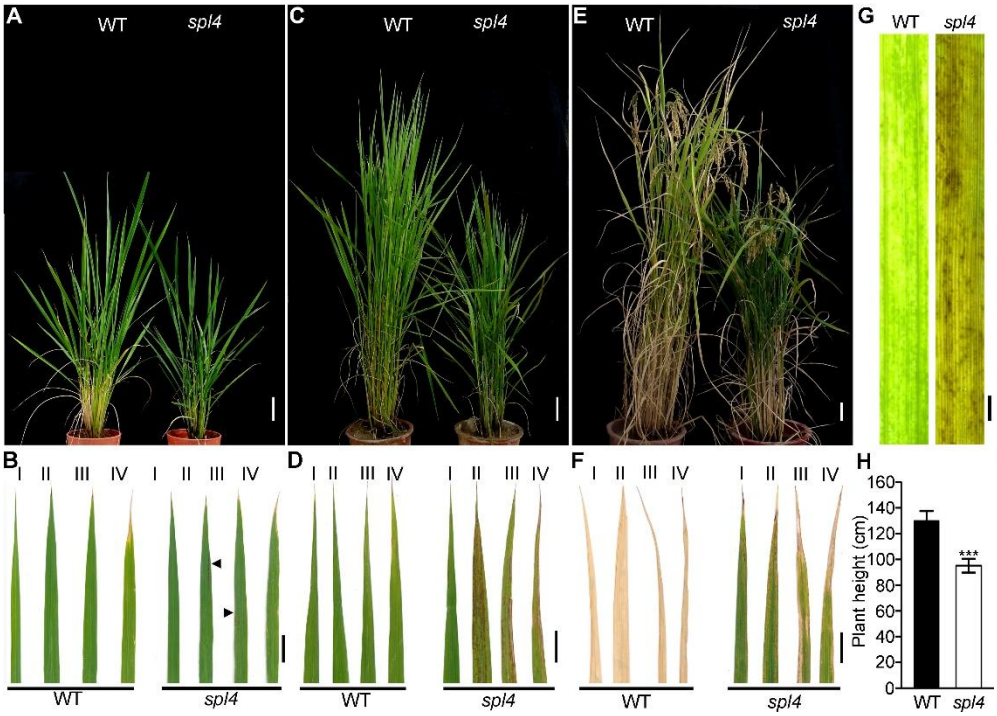

Figure 1. Phenotypic characterization of the *spl4* mutant.

(A-F) Whole plants (A, C, E) and leaf blades (B, D, F) of WT and *spl4* in paddy field. The plants were obtained at 87 (A, B), 118 (C, D), and 162 (E, F) days after sowing. I, II, III, and IV represent 1st leaf, 2nd leaf, 3rd leaf and 4th leaf from the top, respectively. Scale bar = 6 cm (A, C, E), 2 cm (B, D, E). (G) Enlargement of leaf blades of WT and *spl4*. Scale bar = 1cm. (H) Plant height of WT and *spl4* in paddy field. Asterisks are showing statistically significant difference between WT and *spl4* according to Student's t-test (***P < 0.001).

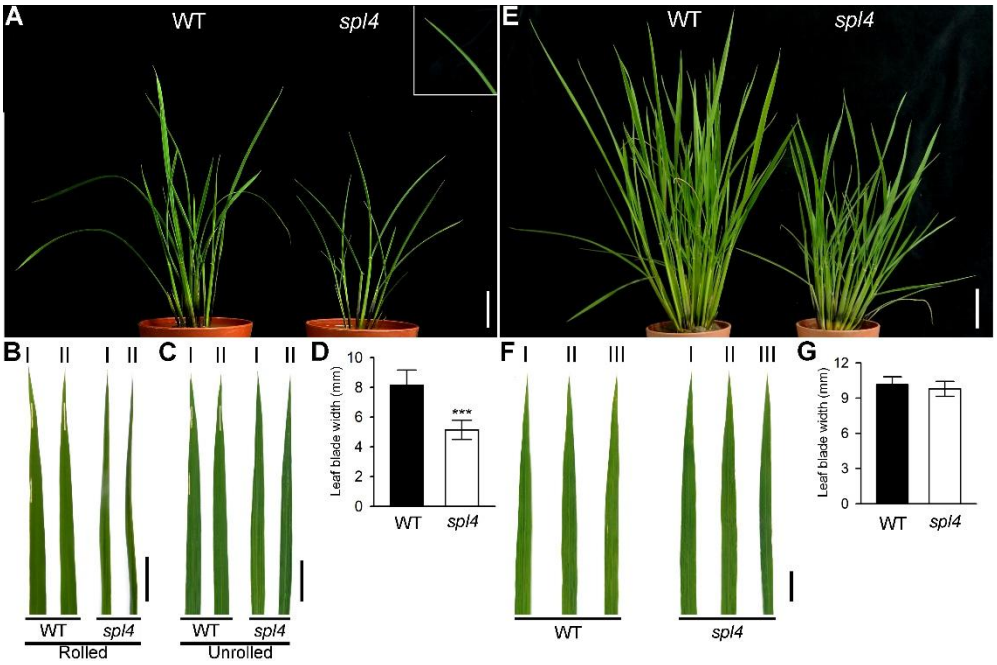

Figure 2. Early phenotypic characterization of the *spl4* mutant.

(A-G) Whole plant pictures (A, E) and leaf blade pictures (B, C, F) of 56- and 74-day-old plants in paddy field. I, II and III represents flag leaf, second leaf and third leaf from the top respectively. Scale bar, A, and E, 5cm. B, C, and F, 2cm. Leaf blade width of 56- and 74-day-old plants in paddy field (D, G). Asterisks are showing statistically significant difference between WT and *spl4* mutant according to Student's T-Test (***P < 0.001)

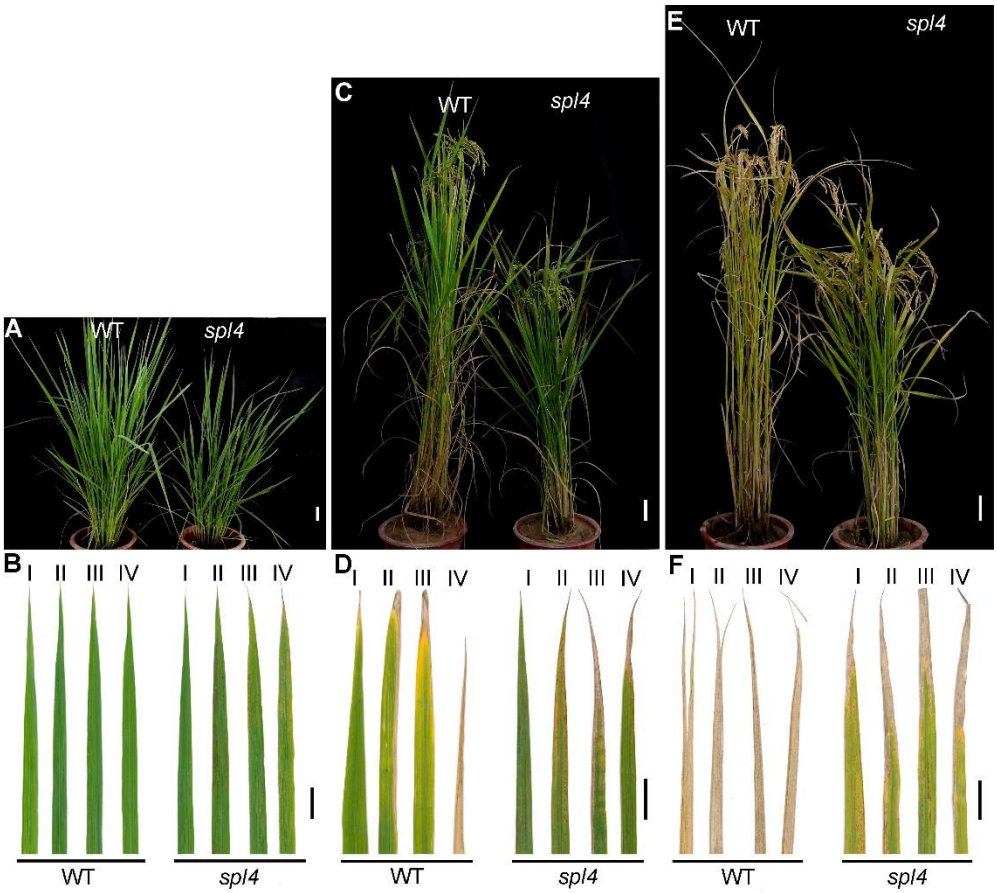

Figure 3. Tillering and heading stage phenotypic characterization of the *spl4* mutant.

(A-F) Whole plant pictures (A, C, E) and leaf blade pictures (B, D, F) of 95-, 147- and 182-day-old plants WT and *spl4* mutant in paddy field. I, II, III and IV represent flag leaf, second leaf, third leaf and fourth leaf from the top respectively. Scale bar, A, 5cm, C and E, 6cm. B, D and E 2cm.

Accumulation of ROS and inducing lesion formation in *spl4* mutants

The *spl4* mutant showed autonomous lesion formation at tillering stage and enhanced greening after heading stage. Commonly, autonomous lesions in leaves are related to ROS [13, 39]. To determine which ROS is accumulating in the *spl4* mutant, we evaluated the accumulation of singlet oxygen ($^1O_2$) by SOSG. We confirmed that $^1O_2$ was accumulated in *spl4* leaves (Fig. 4A). In addition, to verify if there is other accumulating ROS, we further checked DAB staining (Fig. 4B). However, H_2O_2 can be detected by DAB staining, and we found the highly accumulated H_2O_2 in *spl4* mutant (Fig. 4B). To further examine the correlation between ROS and autonomous lesions on *spl4*, we determined the H_2O_2 accumulation of *spl4* leaves from lesion-free phase to lesion formation phase by DAB staining (Fig. 4B). WT and *spl4* in the early stage of tillering did not accumulate the ROS at all (Fig. 4B). At 70 days after sowing, *spl4* still did not show spot formation (Fig. 4B). However, H_2O_2 were stained slightly in *spl4* leaves, despite the absence of the autonomous lesion. After lesion formation in 80 days after sowing plant, *spl4* showed clear lesion formation and severe H_2O_2 accumulation. Finally, before the heading stage when the lesion formation is more severe compared to 80 days after sowing plant, the 125 days after sowing plant showed more accumulation of H_2O_2 (Fig. 4B). This result suggests that the accumulation of ROS is associated with inducing autonomous lesion formation in *spl4*.

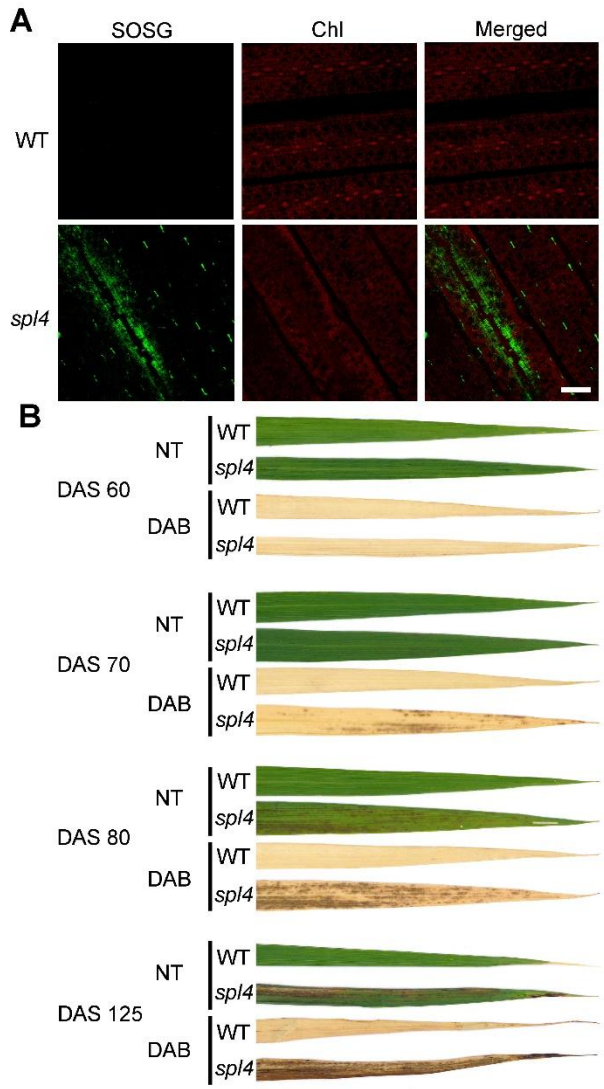

Figure 4. ROS accumulation in *spl4* mutant.

(A) Accumulation of singlet oxygen ($^1O_2$) was detected by SOSG. Scale bar, 5μm. (B) DAB staining of WT and *spl4* mutants grown in NLD paddy field. The samples were obtained at 60, 70, 80, and 125 days after sowing.

Delayed senescence phenotype of *spl4* after lesion formation

As we observed above, another remarkable phenotype of *spl4* was the stay-green phenotype which occurred during leaf senescence (Fig. 1E, F). For the senescence, the lesions on other leaves of *spl4* spread to flag leaf, and *spl4* mutant showed stay-green compared to WT. To further analyze the delayed senescence phenotype of *spl4*, we performed the dark incubation to induce senescence (Fig. 5). After the autonomous lesion formation, the detached leaves of 100-day-old *spl4* showed delayed senescence under dark treatment compared with WT (Fig. 5A). However, the lesion rich region of *spl4* leaves displayed a similar phenotype with WT, in contrast to a non-lesion region of *spl4* leaves (Fig. 5A). Also, a non-lesion region of *spl4* leaves showed higher chlorophyll contents compared to those of WT and lesion rich region of *spl4* leaves (Fig. 5B). By immunoblot analysis, the photosystem proteins such as light-harvesting complex II (Lhcb1, Lhcb2), photosystem II core (D1) and rubisco large subunit (RbcL) were retained in a non-lesion region of *spl4* leaves under dark-induced conditions (Fig. 5C). All these results indicate that the *spl4* senescence is delayed by slower chlorophyll degradation compared with normal senescence.

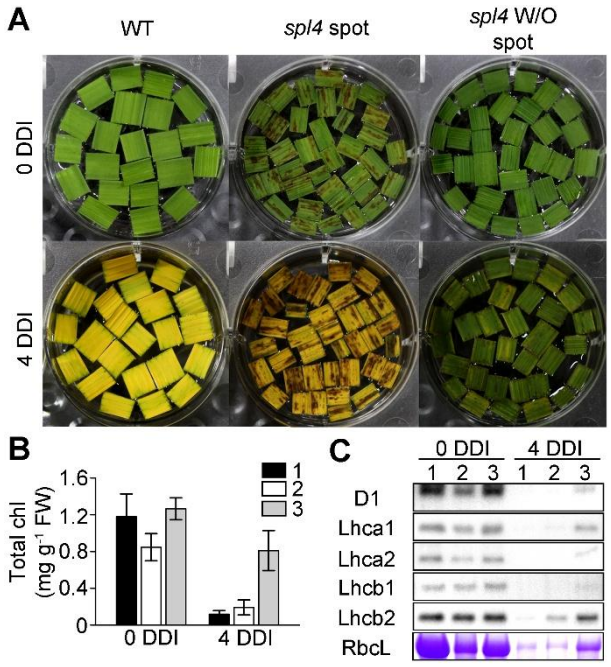

Figure 5. Rice *spl4* mutant showed delayed senescence phenotype during dark-induced condition.

(A) Phenotype of WT and *spl4* leaf discs during dark-induced senescence. Detached leaf discs from 100-day-old WT and *spl4* mutant grown in the greenhouse (Light 14h/Dark 10h) were floated in the MES buffer. *spl4* spot: lesion rich region of *spl4*, *spl4* W/O spot: non-lesion region of *spl4* (B) Total chlorophyll contents of WT and *spl4* after dark-incubation. (C) Immunoblot analysis of photosystem proteins of detached leaf discs. Antibodies against PSI complex subunits (Lhca1, Lhca2) and PSII complex subunits (Lhcb1, Lhcb2, D1) were used for detection. Rubisco large subunit (RbcL) protein was visualized by CBB staining. 1: WT, 2: lesion rich region of *spl4*, 3: non-lesion region of *spl4*

Decreased yield of *spl4* mutants in spite of stay-green phenotype

Next, the stay-green phenotype is important to increase the crop yield production [40]. As the stay-green is one trait to affect in crop yield, we evaluated the yield and yield components of *spl4* in the natural paddy field. We investigated panicles per plant, spikelets per main panicle, seed setting rate, 500-grain weight which are known as major yield components [41], and total yield. Firstly, the agronomic traits were slightly decreased except 500-grain weight (Fig. 6B, E, F, H, Table 2). Also, the main panicle length is considered to one of the yield-related component and one feature of panicle architecture. In *spl4* mutant, the main panicle length was shorter than that of WT (Fig. 6D, G, Table 2). Finally, the yield of *spl4* dropped compared to WT; even so, increased 500-grain weight. Additionally, we found that heading date of *spl4* was approximately 7 days later than that of WT (Fig. 6A, Table 2).

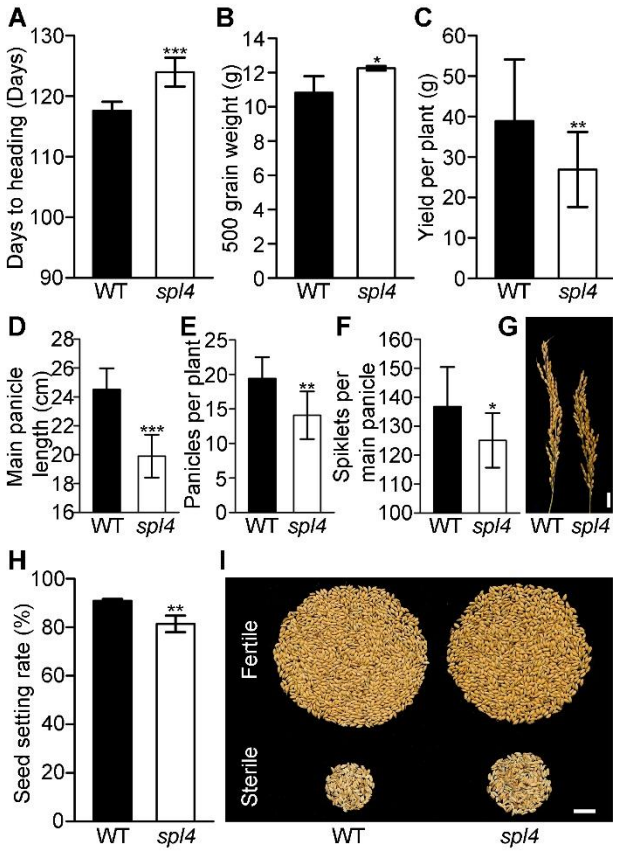

Figure 6. Yield-related agronomic traits of the *spl4* mutant.

Agronomic traits were measured in WT and *spl4* mutant plants grown under NLD in 2015. (A) Days to heading, (B) 500-grain weight, (C) Yield per plant, (D) Main panicle length, (E) Panicles per plant, (F) Spikelets per main panicle and (H) Seed setting rate. 20 plants were used to measure each trait. Student's t-test was used for statistical analysis (*P<0.05, **P<0.01, ***P<0.001). Means and standard deviations are marked as values and vertical bars, respectively. (G) Main panicle from WT and *spl4* mutant. Scale bar = 2cm. (I) Fertile and sterile seeds from the whole plants of WT and *spl4*. Scale bar = 2cm.

Table2. Yield-related agronomic traits of the *spl4* mutant.

Agronomic trait		Average	Standard deviation
Days to heading (days)	WT	117.6	1.47
	spl4	123.9	2.39
500 grain weight (g)	WT	10.8	0.97
	spl4	12.3	0.13
Yield per plant (g)	WT	38.9	15.20
	spl4	26.9	9.28
Main panicle length (cm)	WT	24.5	1.47
	spl4	19.9	1.49
Panicles per plant	WT	19.4	3.06
	spl4	14.1	3.45
Spikelets per main panicle	WT	136.8	13.65
	spl4	125.1	9.42
Seed setting rate (%)	WT	90.9	0.01
	spl4	81.4	0.03

Fine mapping of *spl4*

To map the *spl4* gene, 100 individuals of *spl4* mutant and Milyang23 crossed F2 plants were used. It was reported that mutation of *spl4* is located on chromosome 6 and is a single recessive gene [35]. In 2013, 16 STS and RM markers were used to map and narrow down the *spl4* locus to 1.7Mbp (Fig. 7A). Next year, the 798 plants and more specific 8 STS markers were used for the fine mapping. Finally, the *spl4* locus was confined to 178kb between STS8 and STS9 markers, in the BAC clones, AP000391 and AP000599 (Fig. 7B). We found that thirteen candidate genes are located in this region (Fig. 7C). Based on the whole genome sequencing result and through gene cloning, we identified one base pair mutation at the end of the first intron in LOC_Os06g03940 (Fig. 7D). This gene encodes a spastin which is microtubule-severing protein. It was predicted that the spastin protein has microtubule-interacting and trafficking spastin (MIT spastin) and ATPase associated with wide various of cellular activities (AAA+) superfamily domain (Fig. 7E). To clearly prove the mutation point in *spl4*, we designed the primer to amplified a short region in first to fourth exons in LOC_Os06g03940 (Fig. 7F). It was designed that the amplified fragments had a size of 306bp in WT. However, *spl4* showed multiple fragments and the major fragment of *spl4* had the 13bp deletion at the initiation of the second exon (Fig. 7H). Finally, the *spl4* T-DNA insertion mutants (hereafter *spl4*-KO) showed the same phenotype of *spl4*, suggesting that autonomous lesion formation is caused by

this gene (Fig. 7G).

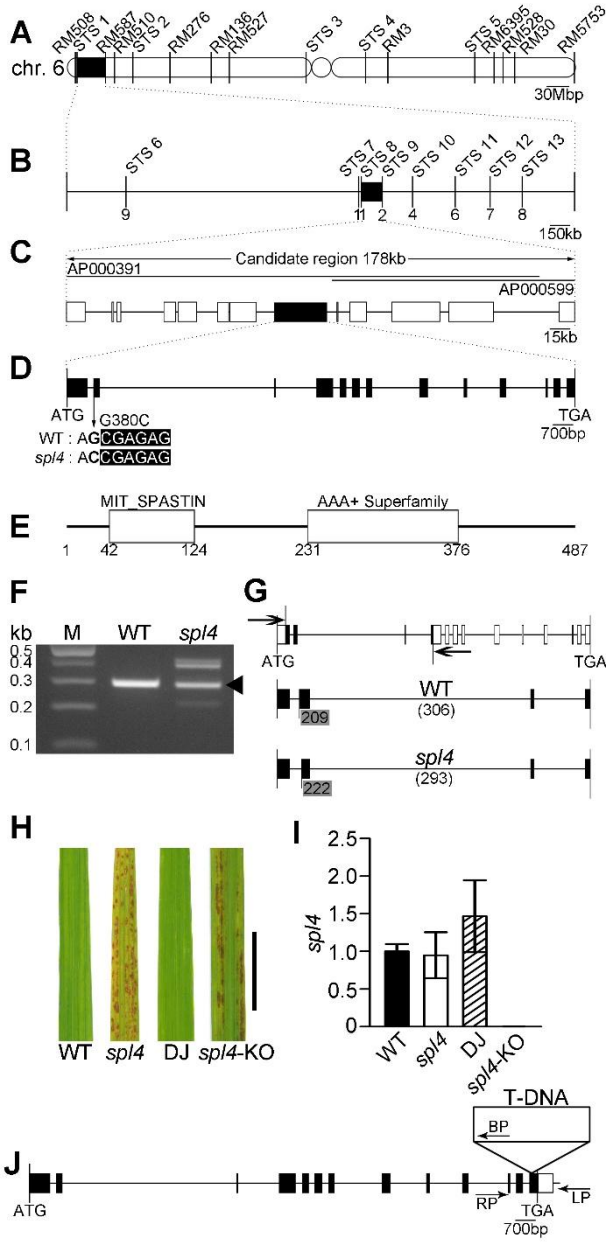

Figure 7. Map-based cloning of *spl4*.

(A) Primary mapping of *spl4* between STS1 and RM587 markers on chromosome 6. (B) Fine mapping of *spl4* between STS8 and STS9 markers. (C) AP000391 and AP000599 (GenBank accession number) BAC clone contigs and putative open reading frames (ORFs) predicted between STS8

and STS9 markers. This data is based on the Rice functional genomic expression database of the Salk Institute Genomic Analysis Laboratory (http://signal.salk.edu/cgi-bin/RiceGE) (D) Structure of the LOC_Os06g03940 which is the candidate gene for *spl4*. (E) Domain structure of LOC_Os06g03940. (F) Splicing variant electrophoresis of WT and *spl4*. (G) Complementation test of *spl4* using T-DNA line, *spl4*-KO. 1: Norin8, 2: *spl4*, 3: DJ (WT of *spl4*-KO), 4: *spl4*-KO. (H) Forward and reverse primer design of splicing variant and its structure of WT and *spl4*. (I) The expression level of OsSPL4 in WT, *spl4*, DJ, and *spl4*-KO. (J) The structure of T-DNA insertion knock out line, *spl4*-KO and its T-DNA insertion site.

SPL4 is localized in linear line shape

To characterize the MIT domain of SPL4, we constructed a *Green Fluorescent Protein (GFP)*-fused *SPL4* vector to examine the subcellular localization of SPL4 protein in rice protoplast. We observed that a luminescence of GFP protein, as a positive control, showed in all over the cytosol and the nucleus, but not overlapped with chlorophyll autofluorescence. In contrast to the result of GFP, the signals of GFP-SPL4 fusion protein showed as speckles in protoplast. GFP-SPL4 was not co-localized with chlorophyll, consistent with only GFP localization (Fig. 8A). To further identify the localization of SPL4 protein, we built another recombinant vector, *Yellow Fluorescent Protein (YFP)-SPL4*. *YFP-SPL4* or only *YFP* vector were delivered to onion epidermal cells by particle bombardment. We also observed many bright speckles in the onion epidermal cell, similar to rice protoplast cells (Fig. 8C). To elucidate the bright speckles of the fusion protein, we applied 4',6-diamidino-2-phenylindole (DAPI) to detect nucleus and zoomed in the nucleus (Fig. 8D). Because one focused layer of zoomed nucleus could not show YFP fluorescence signal, we stacked many layers from various foci and spread out to planar figure (Fig. 8E). YFP-SPL4 proteins were localized as a linear line near the nucleus as the red arrow (Fig. 8E, F). The linear localization can be detected clearly in a 3-dimensional figure (Fig. 8F).

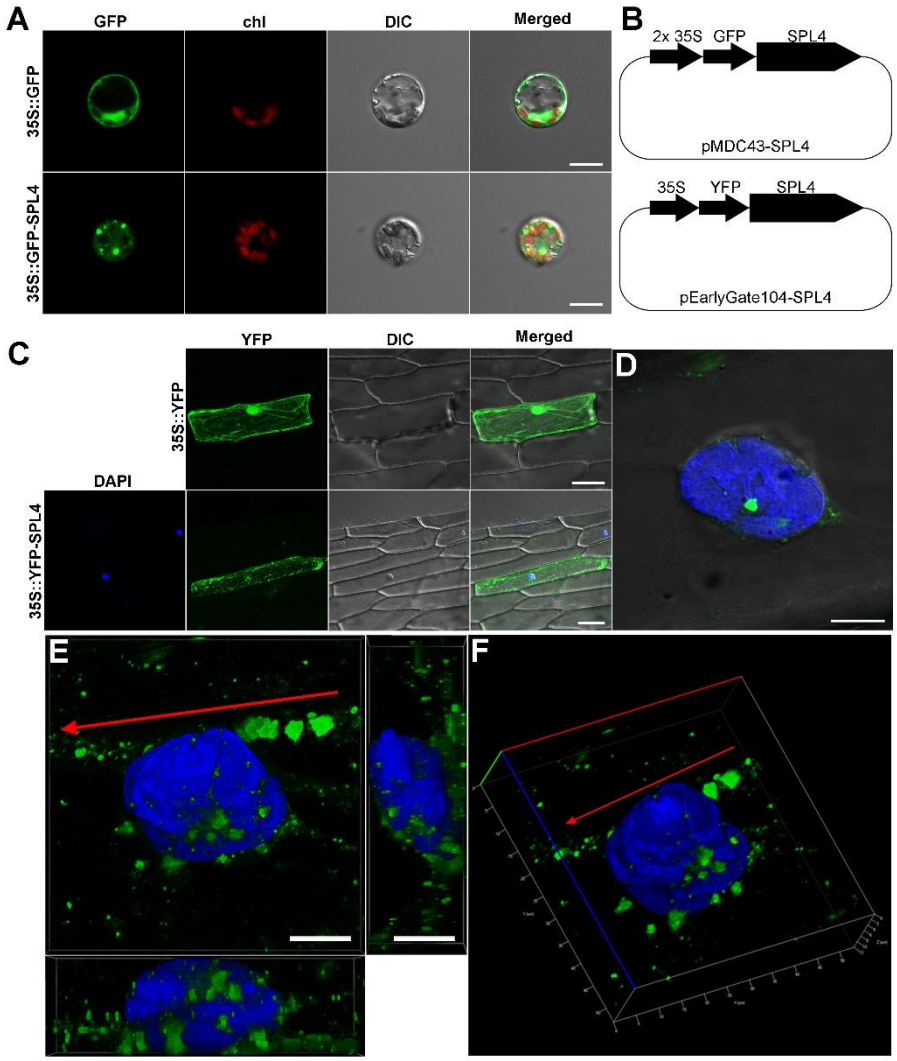

Figure 8. Subcellular localization of SPL4.

(A) Subcellular localization of GFP-SPL4 fusion protein in rice protoplast, analyzed by confocal laser scanning microscopy. Fluorescent (GFP) marked with bright-field, chlorophyll autofluorescence shown with red fluorescence, differential interference contrast (DIC) and merged images are located from left to right. Scale bars, 10μm. (B) The structure of GFP- and YFP- fused vector of pMDC43 and pEarleyGate104. (C) Subcellular localization of YFP-SPL4 fusion protein in onion epidermal layers stained with DAPI, analyzed by

confocal laser scanning microscopy. Blue fluorescent (DAPI), bright-field show the fluorescent (YFP), DIC and merged images are located from left to right. Scale bars, 100μm. Representative confocal images of at least three captures. (D) 40x Zoom image of nuclear in merged image in onion epidermal layers. Scale bars, 10μm. (E) The planar figure of zoom image. The representative planar figure shows an upper image at the center, a front image at the bottom, right side image is located at the center of the image. Scale bars, 10μm. (F) The 3D structure of zoom image.

SPL4 has ATPase activity

Through a computational analysis of protein domain, it was predicted that SPL4 protein has an AAA+ domain (Fig. 7E). For this reason, we examined whether SPL4 has ATPase activity by a biochemical assay of ATPase. To analyze the ATPase activity, we constructed GST-fused SPL4 vector to produce recombinant protein. The predicted size of recombinant protein was 79 kDa, and GST-SPL4 was purified with column affinity chromatography (Fig. 9A, B). By ATPase assay, we found that the recombinant GST-SPL4 protein had ATPase activity, in contrast to the negative controls (Fig. 10A). This result indicates that the GST-SPL4 activity is not performed by GST-tagging, and is specific in this kinetic assay (Fig. 10B). All of this result shows that second domain of SPL4 which is AAA+ domain has ATPase activity.

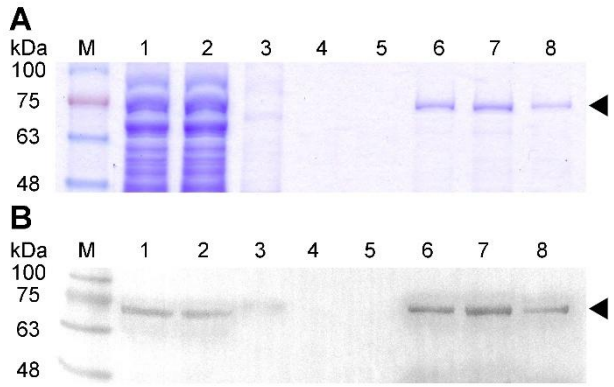

Figure 9. Protein expression of SPL4

(A) SDS-PAGE analysis of GST-SPL4 fusion protein expressed in E.Coli transformant. SDS gel visualized by CBB staining. M:Blueye prestained protein ladder (GeneDirex), Lane1, 2: supernatant, Lane3-5: Washing, Lane6-8: Elution. (B) Western blotting assays of GST-SPL4 fusion protein expressed in E.Coli with mouse anti-GST. M:Blueye prestained protein ladder (GeneDirex), Lane1, 2: supernatant, Lane3-5: Washing, Lane6-8: Elution.

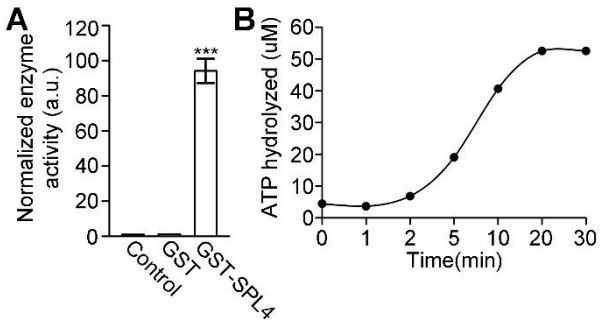

Figure 10. ATPase activity of GST-SPL4.

(A) ATPase activities of purified GST-SPL4 recombinant protein. (B) Endpoint and kinetic measurements of purified GST-SPL4 recombinant protein.

DISCUSSION

The mutagen derived mutant *spl4* shows remarkable phenotype which can be classified as LMM (Fig.1). Many of these mutants were studied previously and several genes involved in spot formation were identified, although the time of occurrence and severity of lesions are variable [42]. It has been reported that almost LMMs shows improved defense mechanism against pathogen [2-4]. Autonomous spot formation in leaves was firstly observed and studied at *Hordeum vulgare* [5], and has been observed over all other spices, such as *Zea mays* [6], *Lycopersicon esculentum* [43] and *Arabidopsis thaliana* [7]. In this study, we determined the mutation on LOC_Os06g03940 in *spl4* mutant by map-based cloning (Fig.7). We found that the SPL4 gene corresponds to LESION MIMIC RESEMBLING (LMR) that was previously reported [1].

By map-based cloning, the mutation point from *spl4* was found (Fig.7A-E). Markers between STS8 and STS9 were thought to be as a candidate region, and with the whole genome sequencing information, we could finally find a spastin expressing *spl4* locus. The spastin encoding gene from *spl4* mutant revealed a single base substitution (G380C) at the first intron. Over the past era, the mechanism of precursor mRNA maturing process has been defined and in this process splicing doner and splicing acceptor is essential to produce a normal mRNA [44]. However, *spl4* gene abolished normal RNA

splicing because of the point mutation at the site of splicing acceptor. Consequently, a primer including that region was designed for clear confirmation and we confirmed multiple splicing variants in *spl4* mutant (Fig. 7F, H). We confirmed SPL4 coding sequences of WT and *spl4* mutant by sequence analysis. The SPL4 sequence of *spl4* mutant showed 13bp deletion at the second exon, which could lead to abnormal translation. Through this result, *spl4* can not produce functional mature mRNA compared with that of WT, resulting in the absence of normal spastin protein.

In this study, we identified the *spl4* gene encodes spastin (Fig. 7). Spastin has been well known as the microtubule severing protein with katanin and fidgetin [30-32]. Generally, among those proteins, the most well-known protein is katanin and second are spastin. Katanin and spastin show the different working model to microtubule [33]. Also, there are two isoforms which are M1 and M87. The difference between these two isoforms is translation initiation site on first exon [45]. Spastin is a major cause of Hereditary spastic paraplegias so-called HSP in human [34]. However, in the plant, which there is no nerve system in organelle so that most of the roles of microtubule severing protein is unclear. In this study, *spl4* showed autonomous lesion formation, late flowering and stay-green phenotype by the mutation of spastin (Fig.1, 5). This suggests that microtubule severing protein is involved in cell death, flowering, and chloroplast degradation pathways. The previous study showed that spastin is involved in cytokinesis, the last step of cell division by interacting with many other proteins like endosomal

sorting complexes required for transport (ESCRT) complex [46]. According to this paper, *spl4* mutant might not perform a normal cell division so that might lead to dwarfism (Fig. 1H). All things are taken together, it might be shown that the phenotype of *spl4* such as cell death, dwarfism and low yield (Fig.1, 6).

The subcellular localization was performed because the first domain of SPL4 was MIT domain. This observation suggests that SPL4 protein might be co-localizes with microtubule because of its MIT domain (Fig. 8F). Microtubules are considered to be an important position for controlling cell stress responses. Microtubules regulate cell stress responses by acting as a scaffold, intracellular trafficking, and transmitting stress signals [47]. It has been reported that the microtubules are important at cellular system working as a trafficking road. Next, the second domain of SPL4 is predicted to AAA+ superfamily domain that indicates a highly conserved sequence through various species. Also, the AAA+ superfamily domain has important roles in many cellular processes. We identified the ATPase activity of SPL4 (Fig. 9), indicating that SPL4 protein has an ATPase activity and possibly function as a microtubule severing protein. Despite many phenotypic characterization and assays, the mechanism of autonomous lesion formation remains to be determined.

Previously, some kinds of LMMs, RLIN1, RLS1 and LM3 genes were identified to encoded coproporphyrinogen III oxidase [48], nucleotide-binding, Apaf-1, R proteins, and Ced-4 (NB-ARC) domain containing protein [49],

uroporphyrinogen decarboxylase (UROD) [50] respectively. However, the exact mechanism of the autonomous lesion formation is still unclear. Many researchers have proposed that the possible mechanism of pathogen resistance in LMMs [51]. In previous models, plant reacts to the pathogen by activating the defense mechanism when they were infected. First, plant recognizes they were infected. Second, the plant sends signals to turn on the defense mechanism and after the signals were sent, such as hyper-resistance (HR) or upregulation of phytoalexin, so called defense phenotypes occurs [52]. Whereas in LMMs, the mutation occurs at the genes involved in pathogen related mechanism, so that mutated genes could not work properly and LMMs phenotypes such as lesion mimic and pathogen resistance might be caused due to the gene mutation which might be involved in pathogen related mechanism [51]. However, the spastin in *spl4* mutant could not function normally so that *spl4* mutant may not severe the microtubule which can derive constant and unnecessary signaling through microtubule that acts as the highway of signaling transduction [47].

Also, in the previous paper the OsACDR1 and *spotted leaf3 (spl3)* mutants showed spontaneous cell death phenotype same as the *spl4* mutant which can be classified to LMM [8, 13]. OsACDR1, OsEDR1, *spl3* were encoding MAPKKK protein according to the previous study [8, 12, 13]. Mitogen-activated protein kinase kinase kinase (MAPKKK) protein is known to activate Mitogen-activated protein kinase kinase (MAPKK) by phosphorylation and the MAPKK phosphorylate the Mitogen-activated protein kinase (MAPK) to make

it active. The final activated protein, the MAPK is the well-known cargo protein of motor protein which moves along through microtubule. These cargo proteins are considered to an important channel in signal transduction pathway as well as diffusion in the cytosol. Therefore, the spontaneous cell death phenotype in *spl3* mutant may due to mutation of a precursor which activating the cargo protein. This mutation may cause difficulty in signal transduction to target site so that the LMM phenotype could appear in these mutants. However, the OsACDR1 over-expression plant showed the same phenotype as mutation plant and this reveals that too much MAPK and no MAPK in the cell could lead to spontaneous cell death [8]. On the other hand, the protein that severe the microtubule, which acts as the way of signal transduction pathway, has been mutated so it may result from too many microtubules in the cell. Too many ways to transmit the signal to the target site may result in spontaneous cell death in *spl4* mutant.

REFERENCES

1. Fekih, R., et al., *The rice (Oryza sativa L.) LESION MIMIC RESEMBLING, which encodes an AAA-type ATPase, is implicated in defense response.* Mol Genet Genomics, 2015. 290(2): p. 611-22.
2. Li, Z., et al., *Fine mapping of the lesion mimic and early senescence 1 (lmes1) in rice (Oryza sativa).* Plant Physiology and Biochemistry, 2014. 80: p. 300-307.
3. Feng, B.H., et al., *Characterization and Genetic Analysis of a Novel Rice Spotted-leaf Mutant HM47 with Broad-spectrum Resistance to Xanthomonas oryzae pv. oryzae.* Journal of integrative plant biology, 2013. 55(5): p. 473-483.
4. Qiao, Y., et al., *SPL28 encodes a clathrin-associated adaptor protein complex 1, medium subunit μ1 (AP1M1) and is responsible for spotted leaf and early senescence in rice (Oryza sativa).* New Phytologist, 2010. 185(1): p. 258-274.
5. Wolter, M., et al., *The mlo resistance alleles to powdery mildew infection in barley trigger a developmentally controlled defence mimic phenotype.* Molecular and General Genetics MGG, 1993. 239(1-2): p. 122-128.
6. Hoisington, D., M. Neuffer, and V. Walbot, *Disease lesion mimics in maize: I. Effect of genetic background, temperature, developmental age, and wounding on necrotic spot formation with Les1.* Developmental biology, 1982. 93(2): p. 381-388.
7. Dietrich, R.A., et al., *Arabidopsis mutants simulating disease resistance response.* Cell, 1994. 77(4): p. 565-577.
8. Kim, J.-A., et al., *Rice OsACDR1 (Oryza sativa accelerated cell death and resistance 1) is a potential positive regulator of fungal disease resistance.* Molecules and cells, 2009. 28(5): p. 431-439.
9. Sun, C., et al., *RLIN1, encoding a putative coproporphyrinogen III oxidase, is involved in lesion initiation in rice.* Journal of Genetics and Genomics, 2011. 38(1): p. 29-37.
10. Wang, J., et al., *Characterization and fine mapping of a light-dependent*

leaf lesion mimic mutant 1 in rice. Plant Physiology and Biochemistry, 2015. 97: p. 44-51.

11. Zeng, Y., et al., *Fine mapping and candidate gene analysis of LM3, a novel lesion mimic gene in rice.* Biologia, 2013. 68(1): p. 82-90.
12. Shen, X., et al., *OsEDR1 negatively regulates rice bacterial resistance via activation of ethylene biosynthesis.* Plant, cell & environment, 2011. 34(2): p. 179-191.
13. Wang, S.-H., et al., *Mutation of SPOTTED LEAF3 (SPL3) impairs abscisic acid-responsive signalling and delays leaf senescence in rice.* Journal of experimental botany, 2015. 66: p. 7045-7059.
14. Zeng, L.-R., et al., *Spotted leaf11, a negative regulator of plant cell death and defense, encodes a U-box/armadillo repeat protein endowed with E3 ubiquitin ligase activity.* The Plant Cell, 2004. 16(10): p. 2795-2808.
15. Yamanouchi, U., et al., *A rice spotted leaf gene, Spl7, encodes a heat stress transcription factor protein.* Proceedings of the National Academy of Sciences, 2002. 99(11): p. 7530-7535.
16. Kasahara, Y., et al., *Involvement of reactive oxygen intermediates in spontaneous and CD95 (Fas/APO-1)–mediated apoptosis of neutrophils.* Blood, 1997. 89(5): p. 1748-1753.
17. Houot, V., et al., *Hydrogen peroxide induces programmed cell death features in cultured tobacco BY-2 cells, in a dose-dependent manner.* Journal of Experimental Botany, 2001. 52(361): p. 1721-1730.
18. Liu, X., et al., *Activation of the jasmonic acid pathway by depletion of the hydroperoxide lyase OsHPL3 reveals crosstalk between the HPL and AOS branches of the oxylipin pathway in rice.* PLoS One, 2012. 7(11): p. e50089.
19. Undan, J.R., et al., *Mutation in OsLMS, a gene encoding a protein with two double-stranded RNA binding motifs, causes lesion mimic phenotype and early senescence in rice (Oryza sativa L.).* Genes & genetic systems, 2012. 87(3): p. 169-179.
20. Jajic, I., T. Sarna, and K. Strzalka, *Senescence, stress, and reactive oxygen species.* Plants, 2015. 4(3): p. 393-411.
21. Thomas, H. and H. Ougham, *The stay-green trait.* Journal of Experimental Botany, 2014. 65(14): p. 3889-3900.

22. Kusaba, M., A. Tanaka, and R. Tanaka, *Stay-green plants: what do they tell us about the molecular mechanism of leaf senescence.* Photosynthesis research, 2013. 117(1-3): p. 221-234.
23. De Keijzer, J., B.M. Mulder, and M.E. Janson, *Microtubule networks for plant cell division.* Systems and synthetic biology, 2014. 8(3): p. 187-194.
24. Mathur, J. and M. Hülskamp, *Microtubules and microfilaments in cell morphogenesis in higher plants.* Current Biology, 2002. 12(19): p. R669-R676.
25. Villari, G., et al., *A direct interaction between fascin and microtubules contributes to adhesion dynamics and cell migration.* J Cell Sci, 2015. 128(24): p. 4601-4614.
26. Gyoeva, F., *The role of motor proteins in signal propagation.* Biochemistry (Moscow), 2014. 79(9): p. 849-855.
27. Verhey, K.J., N. Kaul, and V. Soppina, *Kinesin assembly and movement in cells.* Annual review of biophysics, 2011. 40: p. 267-288.
28. Andreeva, A.V., M.A. Kutuzov, and T.A. Voyno-Yasenetskaya, *Scaffolding proteins in G-protein signaling.* Journal of molecular signaling, 2007. 2(1): p. 1.
29. Alberts, B., et al., *Molecular biology of the cell*. 4th ed.. ed, ed. B. Alberts. 2002, New York: New York : Garland Science, c2002.
30. McNally, F.J. and R.D. Vale, *Identification of katanin, an ATPase that severs and disassembles stable microtubules.* Cell, 1993. 75(3): p. 419-29.
31. Hazan, J., et al., *Spastin, a new AAA protein, is altered in the most frequent form of autosomal dominant spastic paraplegia.* Nat Genet, 1999. 23(3): p. 296-303.
32. Cox, G.A., et al., *The mouse fidgetin gene defines a new role for AAA family proteins in mammalian development.* Nat Genet, 2000. 26(2): p. 198-202.
33. Yu, W., et al., *The microtubule-severing proteins spastin and katanin participate differently in the formation of axonal branches.* Mol Biol Cell, 2008. 19(4): p. 1485-98.
34. Fink, J.K., *The hereditary spastic paraplegias: nine genes and counting.* Arch Neurol, 2003. 60(8): p. 1045-9.
35. Iwata, N., T. Omura, and H. Satoh, *Linkage studies in rice (Oryza sativa L.)*

on some mutants for physiological leaf spots. 九州大学農学部紀要, 1978. 22(4): p. 243-251.

36. Jeon, J.S., et al., *T-DNA insertional mutagenesis for functional genomics in rice.* The Plant Journal, 2000. 22(6): p. 561-570.
37. Jeong, D.H., et al., *Generation of a flanking sequence-tag database for activation-tagging lines in japonica rice.* The Plant Journal, 2006. 45(1): p. 123-132.
38. Porra, R., W. Thompson, and P. Kriedemann, *Determination of accurate extinction coefficients and simultaneous equations for assaying chlorophylls a and b extracted with four different solvents: verification of the concentration of chlorophyll standards by atomic absorption spectroscopy.* Biochimica et Biophysica Acta (BBA)-Bioenergetics, 1989. 975(3): p. 384-394.
39. Chen, X., et al., *SPL5, a cell death and defense-related gene, encodes a putative splicing factor 3b subunit 3 (SF3b3) in rice.* Molecular breeding, 2012. 30(2): p. 939-949.
40. Yoo, S., et al., *Quantitative trait loci associated with functional stay-green SNU-SG1 in rice.* Molecules and cells, 2007. 24(1): p. 83.
41. Xing, Y. and Q. Zhang, *Genetic and molecular bases of rice yield.* Annual review of plant biology, 2010. 61: p. 421-442.
42. Wu, C., et al., *Rice lesion mimic mutants with enhanced resistance to diseases.* Molecular Genetics and Genomics, 2008. 279(6): p. 605-619.
43. Badel, J.L., et al., *A Pseudomonas syringae pv. tomato avrE1/hopM1 mutant is severely reduced in growth and lesion formation in tomato.* Molecular plant-microbe interactions, 2006. 19(2): p. 99-111.
44. Ward, A.J. and T.A. Cooper, *The pathobiology of splicing.* The Journal of pathology, 2010. 220(2): p. 152-163.
45. Claudiani, P., et al., *Spastin subcellular localization is regulated through usage of different translation start sites and active export from the nucleus.* Exp Cell Res, 2005. 309(2): p. 358-69.
46. Vietri, M., et al., *Spastin and ESCRT-III coordinate mitotic spindle disassembly and nuclear envelope sealing.* Nature, 2015. 522(7555): p. 231-5.

47. Parker, A.L., M. Kavallaris, and J.A. McCarroll, *Microtubules and their role in cellular stress in cancer.* Front Oncol, 2014. 4: p. 153.
48. Sun, C., et al., *RLIN1, encoding a putative coproporphyrinogen III oxidase, is involved in lesion initiation in rice.* Journal of Genetics and Genomics, 2011. 38(1): p. 29-37.
49. Jiao, B.B., et al., *A novel protein RLS1 with NB-ARM domains is involved in chloroplast degradation during leaf senescence in rice.* Mol Plant, 2012. 5(1): p. 205-17.
50. Zeng, Y., et al., *Fine mapping and candidate gene analysis of LM3, a novel lesion mimic gene in rice.* Biologia, 2013. 68(1).
51. Bruggeman, Q., et al., *To die or not to die? Lessons from lesion mimic mutants.* Frontiers in plant science, 2015. 6: p. 24.
52. Marino, D., et al., *Arabidopsis ubiquitin ligase MIEL1 mediates degradation of the transcription factor MYB30 weakening plant defence.* Nature communications, 2013. 4: p. 1476.

초 록

본 연구는 감마선을 조사하여 생긴 돌연변이중 벼의 잎에서 자가적인 병반이 생기고 활성산소가 축적되고 지연된 노화를 보이는 돌연변이체중 *SPOTTED LEAF4 (SPL4)*라고 명명된 돌연변이를 이용하여 *spl4* 돌연변이체에서 나타나는 자가적인 병반, 활성산소 축적, 노화 속도 차이를 밝힌 연구이다. 먼저, 논과 온실과 식물생장상 (growth chamber)에서 정상개체와 *spl4* 돌연변이체를 재배한 결과 *spl4* 돌연변이체가 정상개체에 비해 다른 생물학적 감염없이 자가적인 병반이 생기는 것을 확인하였고 개체간 활성산소의 축적도 또한 유의한 차이를 보인것을 확인하였다. 이러한 표현형이 어떠한 유전자에 돌연변이가 생긴것인지 알아보기 위해 map based cloning 을 실시하여 돌연변이가 발생한 유전자를 동정해내었다. 또한 정말 동정해낸 유전자에 의한 표현형인지 알아보기 위해 T-DNA 삽입 돌연변이체를 이용하여 *spl4* 돌연변이체와 표현형을 비교해보았고, 정상개체에 비해 T-DNA 삽입 돌연변이체 또한 *spl4* 돌연변이체와 같은 표현형을 보이는 것을 확인하여 동정해낸 유전자에 의한 표현형임을 확인하였다. 한편, *spl4* 돌연변이체에서 병반 주변에서 활성산소가 축적되는 것을 확인하였고 이를 일정 식물 생장 시간마다 확인한 결과 활성산소가 먼저 축적되고 뒤따라 자가적인 병반이 생기는 것을 확인하였다. 또한, *spl4* 돌연변이체가 정상개체에 비해 노화가 지연되는 것을 확인하였기에 식물체의 잎을 잘라 암처리후 나타나는 표현형과 chlorophylls, chloroplast proteins 함량을 비교하여 정상개체와 *spl4* 돌연변이체간의 유의한 차이가 있는 것을 확인하였다. 마지막으로 *spl4* 돌연변이체에서 돌연변이가 생긴 유전자를 분석한 결과 microtubule-interacting and trafficking spastin 도메인과 ATPase associated with wide various of cellular activities 도메인을 가지고 있는 것으로 확인하였다.